



# The difficulty of estimating the electron transport rate at photosystem I

Riu Furutani<sup>1,2</sup> · Miho Ohnishi<sup>1,2</sup> · Yuki Mori<sup>1</sup> · Shinya Wada<sup>1,2</sup> · Chikahiro Miyake<sup>1,2</sup>

Received: 15 September 2021 / Accepted: 1 November 2021 / Published online: 15 November 2021  
© The Author(s) under exclusive licence to The Botanical Society of Japan 2021

## Abstract

It is still a controversial issue how the electron transport reaction is carried out around photosystem I (PSI) in the photosynthetic electron transport chain. The measurable component in PSI is the oxidized P700, the reaction center chlorophyll in PSI, as the absorbance changes at 820–830 nm. Previously, the quantum yield at PSI [Y(I)] has been estimated as the existence probability of the photo-oxidizable P700 by applying the saturated-pulse illumination (SP; 10,000–20,000  $\mu\text{mol photons m}^{-2} \text{s}^{-1}$ ). The electron transport rate (ETR) at PSI has been estimated from the Y(I) value, which was larger than the reaction rate at PSII, evaluated as the quantum yield of PSII, especially under stress-conditions such as  $\text{CO}_2$ -limited and high light intensity conditions. Therefore, it has been considered that the extra electron flow at PSI was enhanced at the stress condition and played an important role in dealing with the excessive light energy. However, some pieces of evidence were reported that the excessive electron flow at PSI would be ignorable from other aspects. In the present research, we confirmed that the Y(I) value estimated by the SP method could be easily misestimated by the limitation of the electron donation to PSI. Moreover, we estimated the quantitative turnover rate of  $\text{P700}^+$  by the light-to-dark transition. However, the turnover rate of P700 was much slower than the ETR at PSII. It is still hard to quantitatively estimate the ETR at PSI by the current techniques.

**Keywords** Photosynthetic electron transport reaction · Photosystem I · P700 · Y(I)

## Introduction

In the oxygenic photosynthetic organisms, photon energy absorbed by chloroplasts is converted to chemical energy at the thylakoid membrane mainly for driving the Calvin Benson Bassham (CBB) cycle at stroma. This energy-conversion step in photosynthesis is the “photosynthetic electron transport reaction”. At the thylakoid membrane, photon energy absorbed by photosystem II (PSII) induces the photo-oxidation of  $\text{H}_2\text{O}$ , which supplies electrons and  $\text{H}^+$  to the electron transport chain and the luminal side of the thylakoid membrane, respectively. The electrons flow to

ferredoxin (Fd) via plastoquinone (PQ), cytochrome (Cyt)  $b_6f$  complex, plastocyanin (PC), and PSI to reduce  $\text{NADP}^+$  to NADPH catalyzed by Fd-NADP<sup>+</sup> reductase (FNR). At Cyt  $b_6f$  complex,  $\text{H}^+$  is released into the luminal side simultaneously with the oxidation of reduced PQ (or plastoquinol;  $\text{PQH}_2$ ).  $\text{H}^+$  accumulated in the luminal side forms the proton motive force (*pmf*) which drives ATP synthetase to produce ATP from ADP and inorganic phosphate. Produced NADPH and ATP are utilized to assimilate  $\text{CO}_2$  in the CBB cycle. Rubisco catalyzes the oxygenation of RuBP as well as the carboxylation of RuBP, which is the primary reaction of photorespiration. In the photorespiratory pathway, reduced Fd ( $\text{Fd}^-$ ), as well as NADPH and ATP, is also consumed to reproduce RuBP from the primary product, 2-phosphoglycolate. Therefore, these reactions,  $\text{CO}_2$  assimilation and photorespiration, function as the sinks of both electrons and protons produced by the photosynthetic electron transport reaction (Hanawa et al. 2017; Miyake 2020). The photosynthetic electron transport reaction has a mutual correlation with the electron/proton-sink as the electron/proton-source.

✉ Chikahiro Miyake  
cmiyake@hawk.kobe-u.ac.jp

<sup>1</sup> Department of Applied Biological Science, Graduate School for Agricultural Science, Kobe University, 1-1 Rokkodai, Nada, Kobe 657-8501, Japan

<sup>2</sup> Core Research for Evolutional Science and Technology (CREST), Japan Science and Technology Agency (JST), 7 Gobancho, Tokyo 102-0076, Japan

Therefore, the suppression of the CBB cycle directly influences the electron transport reaction.

The possible effect of the suppression of electron/proton-sink activity is the accumulation of electrons in the electron transport chain. Sejima et al. (2014) previously developed the repetitive short pulse (rSP) method in the dark situation which artificially causes the electron accumulation in PSI. rSP-treated plants suffer serious damage to PSI. Further, it turned out that the oxidation of P700 induced by actinic light (AL) illumination suppresses the photoinhibition of PSI by rSP treatments (Sejima et al. 2014). It has been elucidated that the oxidation of P700 is mainly induced by “photosynthetic control” and/or “reduction-induced suppression of electron flow (RISE)” (Furutani et al. 2020a, b; Miyake 2020).

Photosynthetic control is induced by the enhancement of the acidification of the luminal side of the thylakoid membrane. When CO<sub>2</sub> assimilation efficiency is suppressed, the consumption efficiency of H<sup>+</sup> at the lumen of the thylakoid membrane is also suppressed, which lowers the proton conductance (gH<sup>+</sup>) (Wada et al. 2020). This temporal imbalance of H<sup>+</sup> inflow and outflow to/from the luminal side of the membrane enhances the accumulation of H<sup>+</sup> in the thylakoid lumen. Subsequently, the acidic environment in the thylakoid lumen suppresses the electron flow to PSI by down-regulating the efficiency of the oxidation of PQH<sub>2</sub> by Cyt *b<sub>6</sub>f* complex (Nishio and Whitmarsh 1993; Tikkanen et al. 2015) and inducing non-photochemical quenching at PSII (NPQ) (Baker et al. 2007; Kanazawa and Kramer 2002; Tikhonov 2018).

RISE has been observed when both electron/proton-sinks were severely suppressed (Furutani et al. 2020b; Wada et al. 2020). In such situations, the accumulation of electrons in the electron transport chain results in the highly reduced state of the PQ-pool. Over-reduction of the PQ-pool suppresses the oxidation of PQH<sub>2</sub> by Cyt *b<sub>6</sub>f* because of the lack of oxidized PQ for driving the Q-cycle, resulting in the suppression of the electron flow to PSI (Malone et al. 2021; Miyake 2020; Rantala et al. 2020; Shaku et al. 2015; Shimakawa et al. 2018).

It is still under debate how the electron transport reaction is carried out and regulated. Especially, the destinations of the electrons in the CO<sub>2</sub> limited or high light intensity conditions are more complicated. Therefore, simultaneous evaluations of the reaction rates at multiple points in the photosynthetic pathways (i.e. electron transport rate at PSII, the net CO<sub>2</sub> assimilation rate, etc.) would give us important information on the destination of the absorbed photon energy and how plants deal with the excessive light energy. To evaluate the photosynthetic electron transport reaction, two methods are commonly conducted, chlorophyll fluorescence analysis and the absorbance change measurements of the typical light wavelength (Baker 2008; Chance 1972; Klughammer et al.

1990). Chlorophyll fluorescence released from photo-excited chlorophyll *a* in PSII is commonly used for the estimation of the destination of photon energy absorbed in PSII (Baker 2008). Yield II [Y(II)], a parameter of the effective quantum yield of PSII, is obtained as the variable chlorophyll fluorescence under AL by applying saturated pulse (SP) illumination (10,000–20,000 μmol photons m<sup>2</sup> s<sup>-1</sup>) which instantaneously makes a full-reduced situation of electron carriers at the acceptor side of PSII. There is extensive research on Y(II) and gas-exchange analysis, and it has been confirmed that Y(II) and electron consumption rate of both CO<sub>2</sub> assimilation and photorespiration, estimated by gas-exchange technique, have linear relationships originated at almost zero (Driever and Baker 2011; Genty et al. 1990; Ghashghaie and Cornic 1994; Ruuska et al. 2000). Therefore, it can be said that Y(II) is one of the reliable parameters for estimating the potential of electron transport reactions. Concerning the PSI, absorbance changes depending on the P700<sup>+</sup> (820–830 nm) have been used for the analysis (Klughammer and Schreiber 1991; Schreiber et al. 1988). Yield I [Y(I)], the effective quantum yield of PSI, is also estimated by applying SP illumination to leaf samples (Klughammer and Schreiber 1994). In this case, Y(I) shows the ratio of photo-oxidizable P700 by SP illumination to total P700 content. Previously, Y(I) and Y(II) are used for the estimation of electron transport rate by multiplying them by the photosynthetic photon flux density and the coefficient for the deviation ratio of light energy to each photosystem (often 0.4–0.45 are used for) (Baker et al. 2007; Miyake et al. 2004). Comparing the electron transport rate (ETR) estimated from Y(II) and Y(I), it is often observed that ETR at PSI [ETR(I)] is higher than ETR(II) (Brestic et al. 2016; Makino et al. 2002; Miyake et al. 2004, 2005, 2015; Munekage et al. 2002; Zhang et al. 2019; Zivcak et al. 2013). This phenomenon is more often observed in CO<sub>2</sub>-limited conditions or high light intensity regions, where the oxidation level of P700 increases. Therefore, it has been estimated that some kinds of mechanisms, which caused the excessive electron flow at PSI, contributed to the oxidation of P700 (Kono and Terashima 2016; Livingston et al. 2010; Miyake et al. 2004, 2005; Munekage et al. 2004; Yamori et al. 2016; Zivcak et al. 2013).

Previously, Kadota et al. (2019) and Shimakawa and Miyake (2021) reported that Fd reduction/oxidation rate under steady-state photosynthesis showed linear relationships with Y(II) originating at zero. If both Y(I) and Y(II) quantitatively reflected the electron flow at PSI and PSII, respectively, one possible reason for the larger Y(I) values would be that electrons were recycled within PSI, called “charge recombination” (Kadota et al. 2019). Another possible explanation is the “overestimation of Y(I)”.

In the present research, we conducted the Y(I) estimation by SP-method in the darkness to simplify the situations (i.e. no need to concern any regulations of the electron transport

and electron consumption capacities of Calvin cycle). By applying far-red light (FR) illumination which specifically photo-excites PSI, we imitated the PSI-donor side limiting situation, where only PC (or the donor side of PSI) was oxidized. In the PC-oxidized situations, the  $Y(I)$  values were significantly higher than that in the dark-adapted state, which indicated the PSI-donor side limitation could cause the misestimation of  $Y(I)$  value. Previously, it was reported that in proton gradient regulation 5 protein (PGR5) deficient mutants showed closer/lower  $Y(I)$  values when compared to  $Y(II)$  under steady-state photosynthesis. Even in the previously isolated PGR5-defective mutant *pgr5<sup>hope1</sup>*, which showed lower  $Y(I)$  than  $Y(II)$ , the misestimation of  $Y(I)$  was observed as in WT under the artificial PC-limiting situation. The result from the mutants *paal-7/pox1*, which showed a decreased amount of PC, strongly supported the suggestion that the PSI-donor side limitation of the electron flow would cause the misestimation of  $Y(I)$  value. We tried another method to estimate the reduction rate of P700 in PSI by dark-interval relaxation kinetics (DIRK) analysis (Sacksteder and Kramer 2000) using the Dual-KLAS/NIR. However, the turnover rate of P700 estimated from this method was significantly smaller, compared to ETR(II). These results suggested that the equilibrium reaction of both Cyt *f*-PC and PC-P700 electron transportation steps cannot be ignored in vivo. In the end, we revisit the research by Sacksteder and Kramer (2000), which has applied the summation method to the electron transport reaction from Cyt *f* to P700.

## Materials and methods

### Plant materials and growth condition

Plants of *Arabidopsis thaliana* wild-type (gl-1) and the mutants, *pgr5<sup>hope1</sup>* and *paal-7/pox1*, were grown in a controlled chamber (10 h light at 25 °C/14 h dark at 22 °C; 100–150  $\mu\text{mol photons m}^{-2} \text{s}^{-1}$  of light intensity; 50–55% of relative humidity). Seeds were planted in pots that contained a 1:1 mix of vermiculite and seeding-culture soil (TAKII Co., Ltd.). Plants were watered every 2–3 days and 1000-fold diluted Hyponex solution (Hyponex, Osaka, Japan) was used once, 3 weeks after the seeding. Measurements were conducted using the rosette leaves of the plants 5 weeks after germination.

Wheat (*T. aestivum* L. cv Norin 61) plants were grown in the experimental field of Kobe University (34°44' N, 135.14' E) in April 2021. The width and length of the fields were 4.3 m  $\times$  4.0 m, and there were three ridges in the field. The height of the ridge was approximately 20 cm. Wheat plants were planted at a density of 35 plant  $\text{m}^{-2}$ . Before seeding, we used urea, superphosphate, and potassium chloride fertilizer

as basal fertilizers (60 kg  $\text{ha}^{-1}$  as N,  $\text{P}_2\text{O}_5$ ,  $\text{K}_2\text{O}$ ). After seeding, liquid fertilizer of inorganic nutrients (natural mineral-1, Sanei Co., Ltd., Japan) was applied every 3 days for the first week, and once a week for the next 3 weeks, and then every 3 weeks until 3 months from the germination. For the measurements, we used the second leaves from the top of 4–5 weeks-old wheat plants.

### Measurements of the absorbance changes of the oxidized P700 (P700<sup>+</sup>), oxidized PC (PC<sup>+</sup>), reduced Fd (Fd<sup>-</sup>), and the chlorophyll fluorescence

The redox states of the P700, PC, and Fd were estimated from the absorbance changes of the four dual-wavelength (785–840 nm, 810–870 nm, 870–970 nm, 795–970 nm) measured by Dual-KLAS/NIR. These absorbance changes were deconvoluted into the signals for P700<sup>+</sup>, PC<sup>+</sup>, and Fd<sup>+</sup> by referring to the differential model plot obtained before the measurements as described previously (Klughammer and Schreiber 2016). We determined the maximal reduction/oxidation-dependent absorbance changes of P700<sup>+</sup>, PC<sup>+</sup>, and Fd<sup>-</sup> to convert all the signals into relative values.

The kinetics of three components during the saturated pulse illumination (SP; 10,000  $\mu\text{mol photons m}^{-2} \text{s}^{-1}$ , 300 ms of duration) was measured in three situations (Fig. 1); (I) dark-adapted state, (II) 3 s after the 10 s of far-red illumination (740 nm) and single turnover illumination, where PC was still oxidized while almost all of P700<sup>+</sup> turned back to the ground state, and (III) 13 s after the second situation, where the redox states of the three components went back to the dark-adapted state. We considered the maximal oxidation peak values of P700<sup>+</sup> during SP illumination as  $Y(I)$  in the text.

The initial reduction/oxidation rate of P700<sup>+</sup> under steady actinic light (AL; 1,850  $\mu\text{mol photons m}^{-2} \text{s}^{-1}$ ) was measured by dark-interval relaxation analysis as described in Sacksteder and Kramer (2000), changing the ambient partial pressure of  $\text{CO}_2$  (40, 30, 20, 10, 5 Pa) under photorespiratory conditions (21 kPa  $\text{O}_2$ ). We manually drew lines of the initial linear phases of the reduction of P700<sup>+</sup> and the slope of the line was considered as the relative initial reduction rate of P700<sup>+</sup>. We determined the amount of P700 in the measured leaves on the leaf area basis by the method below and obtained the turnover rate of P700 by multiplying the relative initial redox rate ( $\% \text{s}^{-1}$ ) and the amount of P700 ( $\mu\text{mol m}^{-2}$ ) together.

Simultaneously, chlorophyll fluorescence was measured by the same instrument. Weak measuring light (540 nm) was applied to the wheat leaves and obtained the following parameters; the maximal quantum yield of PSII (Fv/Fm),  $Fv/Fm = (Fm - Fo)/Fm$ ; the effective quantum yield of PSII [ $Y(II)$ ],  $Y(II) = (Fm' - Fs)/Fm'$ ; the non-photochemical quenching (NPQ),  $NPQ = (Fm/$

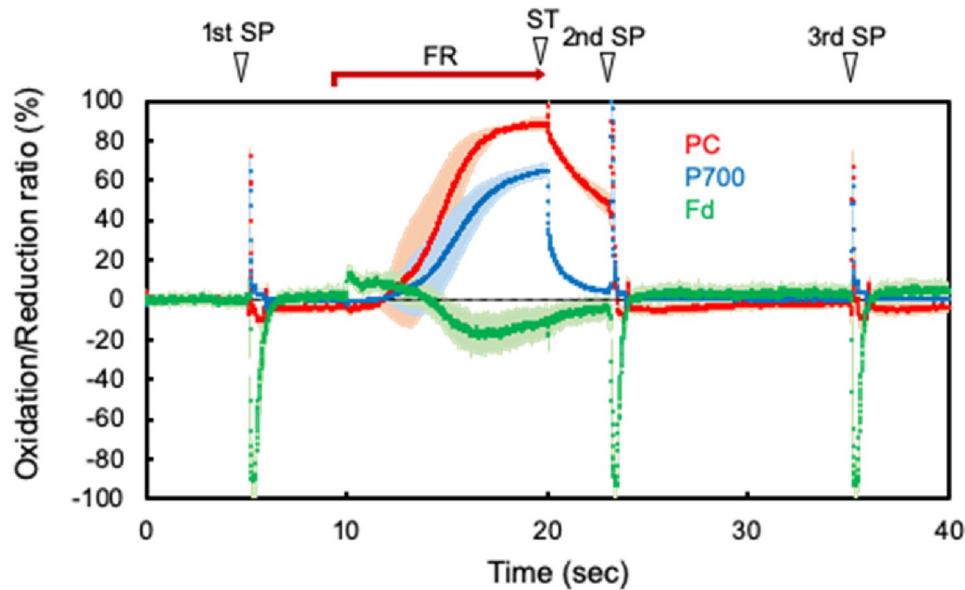


**Fig. 1** The scheme and the result of the Y(I)-estimation experiments. The result from the wild-type *A. thaliana* is shown. The estimation of Y(I) was conducted as follows; (I) the first saturated pulse (SP) application at 5 s under dark-adapted state. (II) the application of the 10 s of far-red light (740 nm) illumination and single turnover (ST) illumination (50  $\mu$ s) was applied at 20 s. (III) The second SP illumination 3 s after the ST illumination (at 23 s). (IV) The third SP application 13 s after the second SP illumination (at 35 s). The relative reduc-

tion/oxidation states of P700 (blue symbols), plastocyanin (PC) (red symbols), and ferredoxin (Fd) (green symbols) were shown with SD (thin colored lines of each component). The maximal redox changes of P700, PC, and Fd were determined as shown in Supplemental Figure S4 and S5, and each signal was normalized by those values. The number of biological replicates is 6 and each signal was obtained by averaging 6 sets of measurements

$F_m' - 1$ .  $F_m$  and  $F_m'$  was the maximal fluorescence intensity by applying the saturated pulse illumination (SP; 15,000  $\mu$ mol photons  $m^{-2} s^{-1}$ , 300 ms of the duration) under dark and AL, respectively.  $F_o$  and  $F_s$  were the stationary levels of the chlorophyll fluorescence under dark and AL, respectively. Using Y(II), we calculated the electron transport rate at PSII (ETR<sub>II</sub>) as follows;  $ETR_{II} = Y(II) \times \alpha \times PPFD$ .  $\alpha$  is the deviation ratio of the light energy to PSII. We assumed the equal distribution of the light energy to two photosystems, and 0.45 was used for  $\alpha$  value. PPFD is the photosynthetic photon flux density.

We also conducted A-Ci analysis measuring the chlorophyll fluorescence and P700<sup>+</sup> absorbance changes at 830 nm in WT, *pgr5<sup>hope1</sup>*, and *paa1-7/pox1* by Dual-PAM instrument. The photosynthetic parameters for the electron transport reaction at PSI were obtained as follows; the maximal photo-oxidizable P700,  $P_m$ ; the photo-oxidizable P700 under AL,  $Y(I) = P_m'/P_m$ ; the existence ratio of oxidized P700,  $Y(ND) = P/P_m$ ; the non-photo oxidizable and not oxidized P700,  $Y(NA) = (P_m - P_m')/P_m$ .  $P_m$  and  $P_m'$  are the maximal absorbance changes induced by applying SP under dark and AL, respectively, and  $P$  is the stationary levels of the P700<sup>+</sup> absorbance signal under actinic light.

## Gas exchange analysis

Gas exchange analysis was carried out by LI-7000 (LI-COR, Lincoln, USA). The changes of the partial pressure of CO<sub>2</sub> and H<sub>2</sub>O in the 3010-Dual gas exchange chamber (Heinz Walz, Effeltrich, Germany) were measured. In the measuring chamber, the ambient air was saturated with water vapor at  $16 \pm 0.1$  °C and the temperature was maintained at  $25 \pm 0.5$  °C (55–60% of the relative humidity). We measured the respiration rate (R<sub>d</sub>), assumed to be constant regardless of the supply of the light, and the CO<sub>2</sub> absorption rate (A). We assumed the net CO<sub>2</sub> assimilation rate as  $A + R_d$ .

## Isolation of the thylakoid membrane from wheat leaves

A raw leaf blade (SPAD > 40) from the top of the wheat plants was sampled and scanned by an image scanner. The analysis of the images was conducted by Image J (ver.1.53). The leaf samples were homogenized in 50 mM sodium phosphate buffer (pH 7.2) containing 120 mM 2-mercaptoethanol, 1 mM iodoacetic acid, and 5% (v/v) glycerol at a leaf: buffer ratio of 1: 9 (g mL<sup>-1</sup>) in a chilled mortar and pestle. 50  $\mu$ L of the suspension was used for the determination of the chlorophyll content. Absorbance changes at 720,



663, and 645 nm were measured to calculate the chlorophyll content by the Arnon method. The rest of the homogenate was centrifuged at 14,000 rpm for 10 min at 4 °C. The pellet was resuspended well in 1 mL of the homogenizing buffer (0.4 M sucrose, 2 mM MgCl<sub>2</sub>·6H<sub>2</sub>O, 10 mM NaCl, 50 mM HEPES, pH was adjusted to 7.5 by KOH) containing 1 mM ascorbate. The homogenate was applied to 1 mL of percoll solution (40% (v/v) percoll, 50 mM HEPES, 0.53 M sorbitol, 1 mM MgCl<sub>2</sub>·6H<sub>2</sub>O, 2 mM EDTA-Na, 10 mM NaCl, 1 mM MnCl<sub>2</sub>, and pH was adjusted to 7.6 by KOH) and centrifuged at 14,000 rpm for 10 min at 4 °C. The fraction of the thylakoid membrane was extracted and resuspended in the homogenized buffer without ascorbate after washing by the same buffer. The chlorophyll content of this solution was also measured by the same method above.

### Determination of the amount of P700 in leaves

The solution of the isolated thylakoid was applied to the measuring cell with 20 μmol methyl-viologen, adjusting the chlorophyll concentration to 40 μg mL<sup>-1</sup>. The absorbance changes of the two dual-wavelengths (820–870 nm and 870–965 nm) were measured using Dual-KLAS/NIR. The maximal absorbance changes of these two dual-wavelengths were obtained by applying ST illumination under the 10 s of FR illumination. The maximal absorbance changes of 820–870 nm ( $\Delta A_{820-870}$ ) and 870–965 nm ( $\Delta A_{870-965}$ ) were calculated to determine the concentrations of P700 and PC as follows;

$$\begin{bmatrix} [\text{PC}] \\ [\text{P700}] \end{bmatrix} = \begin{bmatrix} \epsilon_{\text{PC}(820-870)} & \epsilon_{\text{PC}(820-965)} \\ \epsilon_{\text{P700}(820-870)} & \epsilon_{\text{P700}(820-965)} \end{bmatrix}^{-1} \begin{bmatrix} \log(e) \times \Delta A_{820-870} \\ \log(e) \times \Delta A_{820-965} \end{bmatrix}$$

$\epsilon$  is the molecular extinction coefficient and 0.44 for  $\epsilon_{\text{PC}(820-870)}$ , 7.35 for  $\epsilon_{\text{PC}(820-965)}$ , 1.34 for  $\epsilon_{\text{P700}(820-870)}$ , and 10.3 for  $\epsilon_{\text{P700}(820-965)}$  were used as previously described (Kirchhoff et al. 2004; Klughammer and Schreiber 1991; Oja et al. 2003; Rott et al. 2011). Minus one in the super-script of the matrix shows the inverse matrix of the shown matrix.  $\Delta A_{820-965}$  was calculated as the sum of  $\Delta A_{820-870}$  and  $\Delta A_{870-965}$ . The amount of the P700 was calculated on a leaf-area basis.

### Western blot

Western blot analysis was carried out using the antibody against plastocyanin purchased from Agrisera (Vännäs, Sweden). Leaf samples (approximately 10 cm<sup>2</sup> leaf section) were derived from the 5 week-old *A. thaliana* wild-type and *paal-7/pox1* mutants grown in the condition described above. The leaf samples were homogenized in 50 mM sodium phosphate buffer (pH 7.2) containing 120 mM 2-mercaptoethanol,

1 mM iodoacetic acid, and 5% (v/v) glycerol at a leaf: buffer ratio of 1: 5 (g mL<sup>-1</sup>) in a chilled mortar and pestle. The suspensions were centrifuged at 13,000 rpm for 10 min and the supernatants were mixed with the same amount of the SDS buffer containing 200 mM Tris-HCl (pH 8.5), 2% (w/v) SDS, 20% (v/v) glycerol, and 5% (v/v) 2-mercaptoethanol. The solution was boiled for 3 min, and 10 μL of the protein samples were loaded onto the precast gels with Tris-glycine buffer containing 250 μM Tris, 1.92 mM glycine, and 0.1% (w/v) SDS. Proteins were blotted onto a polyvinylidene difluoride membrane. After the blotting, the membrane was washed three times by the blocking buffer, containing 10 mM sodium-phosphorus solution (pH 7.2), 0.9% (w/v) NaCl, 0.05% (v/v) Tween-20, and 0.5% (w/v) skim-milk, and incubated by the primary antibody solution (blocking buffer with 0.05% NaN<sub>3</sub> and 4,000-fold diluted anti-PC antibody solution) overnight at 25 °C. After the incubation in the secondary antibody solution (blocking buffer with 20,000-fold diluted anti-antibody solution) for 1 h, the PC was detected using the enhanced chemiluminescence substrate from Thermo fisher scientific (Massachusetts, USA). The images of the gels were analyzed by Image J (ver. 1.53) and the intensities of PC bands on the leaf area basis were compared between wild-type and *paal-7/pox1* mutants.

### Statistical analysis

The statistical analysis of the corresponding data in Figs. 3, 4, and Figs. S3 and S5 (Welch's *t* test) was performed using

the commercial Microsoft Excel for Mac (ver. 16.16.27). The number of biological replicates was 4–6.

## Results

### The kinetics of oxidized P700 while the saturated pulse illumination differs depending on the oxidation levels of PC

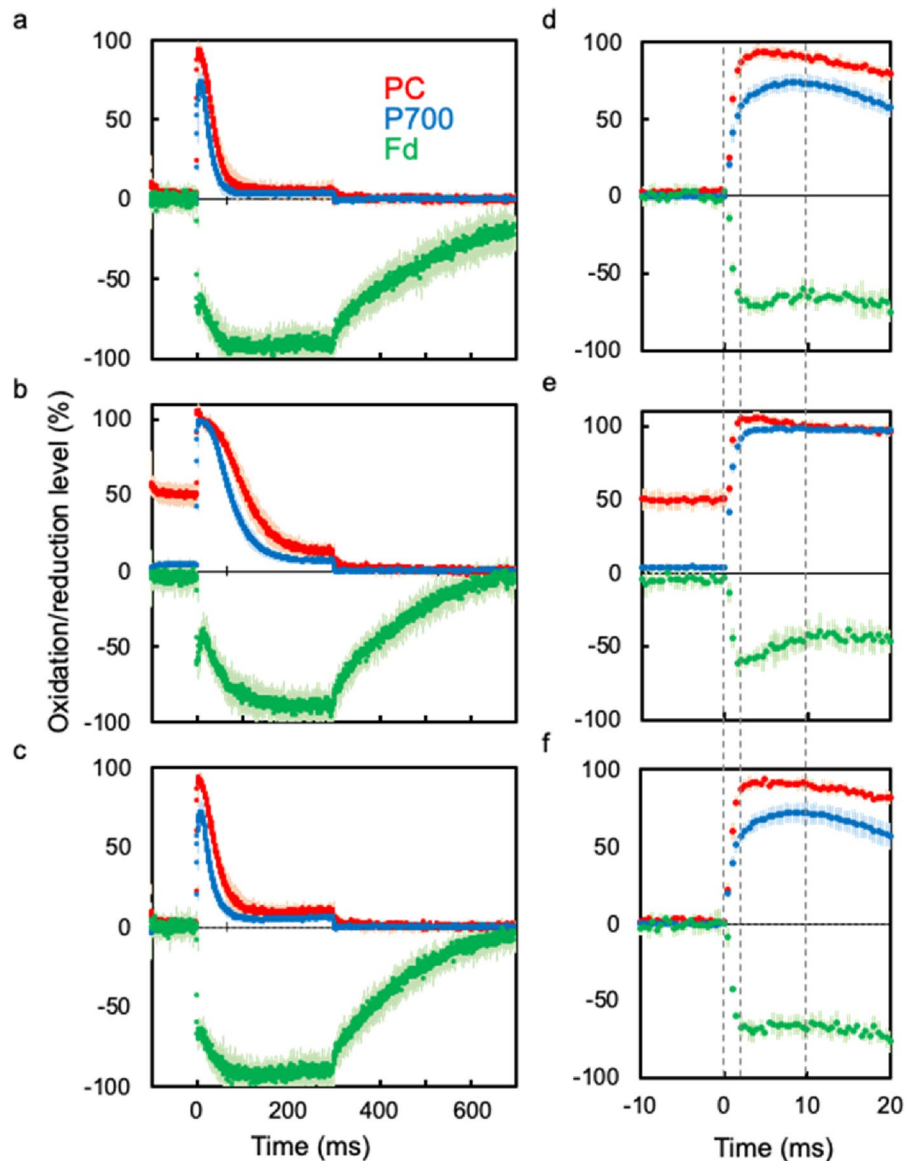
To examine whether *Y(I)* correctly reflects the quantum yield of PSI or not, we carried out the following treatments according to the method described in Furutani et al. (2020a), using *A. thaliana* wild-type (Fig. 1). I, the first estimation of *Y(I)* by applying SP (10,000 μmol photons m<sup>-2</sup> s<sup>-1</sup>, 300 ms duration) was carried out under dark at 5 s; II, far-red light illumination (740 nm) for 10 s and single turnover flash (50 μs) was applied; III, 3 s after the ST flash, where almost all of P700<sup>+</sup> returned to the ground state while PC was still

oxidized, the second estimation of  $Y(I)$  by SP illumination was carried out; IV, the third estimation of  $Y(I)$  was conducted under dark at 35 s, where all electron carriers returned to the same state as the dark-adapted state.

During the first SP illumination under the dark-adapted state, the oxidation kinetics of P700 within 10 ms is divided into two phases (Fig. 2d). In the fast phases ( $\sim 2$  ms), the charge separation of P700 occurred extracting the electrons from PC and Cyt *f*. The charge separation of P700 occurred more rapidly than the donation of electrons from the donor side, resulting in the oxidation of P700 to nearly 60%. In the slow phases, P700 was slowly oxidized and showed the peak (70–75% oxidized) around 10 ms (Fig. 2d). This retarded oxidation of P700 showed that the photo-reduction/oxidation cycle of P700 was driving even within a few milliseconds during the SP illumination. After the peak at 10 ms, the ratio

of  $P700^+$  decreased sharply and reached nearly zero within 100 ms (Fig. 2a). This drastic decrease of  $P700^+$  starting at 10 ms after the SP application was due to the flood of electrons from PSII while photo-activation of FNR did not occur and therefore the acceptor side of PSI could not release electrons downstream. The time scale of the reduction of  $P700^+$  roughly corresponded to the half-time of the oxidation of  $PQH_2$  by Cyt *b\_6/f* complex (10–20 ms) (Hope 1993). Following the previous method for estimating  $Y(I)$ , the  $Y(I)$  in this situation would be 0.7–0.8 which roughly corresponded to the  $F_v/F_m$  value ( $=0.782 \pm 0.006$ ;  $n=6$ ) (Fig. 3). PC was rapidly oxidized to 90% within 2 ms during the SP illumination (Fig. 2d). After the peak around 2–3 ms, PC was slightly reduced but kept oxidized to 10 ms. In this phase, PC would have donated electrons to P700 as soon as it extracted electrons from Cyt *f*, resulting in the stable

**Fig. 2** The kinetics of the oxidized P700 ( $P700^+$ ; blue symbols), oxidized plastocyanin ( $PC^+$ ; red symbols) and reduced ferredoxin ( $Fd^-$ ; green symbols) with SD (thin colored lines of each component) in wild-type *A. thaliana* during the first (a, d), second (b, e) and third (c, f) saturated pulse (SP) applications. SP illumination ( $10,000 \mu\text{mol photons m}^{-2} \text{s}^{-1}$ ) was applied from 0 to 300 ms. The gray dashed lines in the panel d–f showed 0 ms, 2 ms, and 10 ms from the SP application, respectively. The maximal redox changes of P700, PC, and Fd were determined as shown in Figs. S4 and S5, and each signal was normalized by those values. The number of biological replicates is 6 and each signal was obtained by averaging 6 sets of measurements



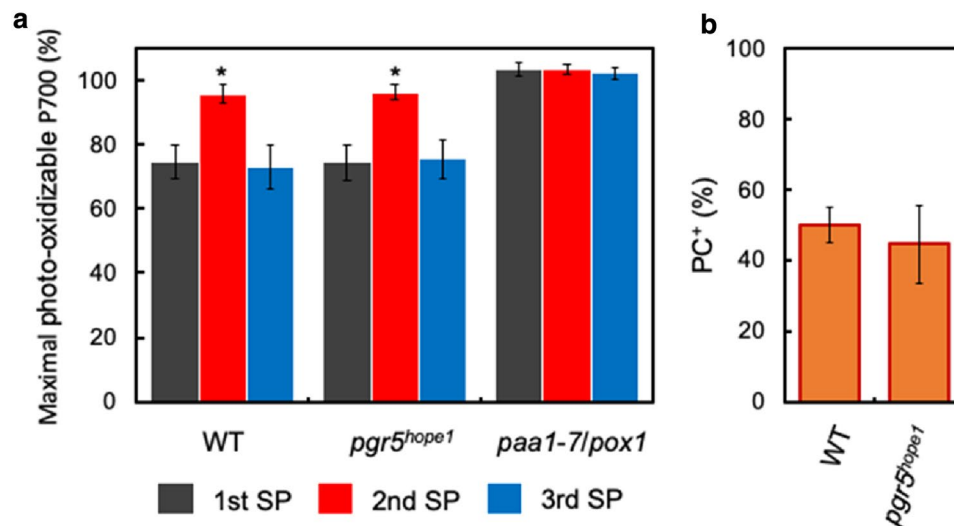


**Fig. 3** The maximal photo-oxidizable P700 by three saturated pulse (SP) illuminations ( $\approx Y(I)$ ) in wild-type (black), *pgr5<sup>hope1</sup>* (blue), and *paa1-7/pox1* (red) and the oxidation levels of PC (orange) just before the second SP applications are shown.  $Y(I)$  was determined as the peak values of  $P700^+$  during SP illumination. Data are shown as average values with SD. The maximal redox changes of P700, PC, and Fd were determined as shown in Figs. S4 and S5, and each signal

was normalized by those values. The oxidation levels of *paa1-7/pox1* mutants are not shown because the maximal photo-oxidizable PC was not detectable. The asterisks indicate that it was statistically different ( $p < 0.01$ ) when compared to the value in the first estimation of  $Y(I)$  in each phenotype. The number of biological replicates is 6 and each signal was obtained by averaging 6 sets of measurements

oxidation levels of PC around 90%. After the 10 ms from SP application, PC was also rapidly fully reduced within 100 ms as P700 (Fig. 2a). Fd was rapidly reduced by the SP illumination and showed the first peak at 2 ms (65–70% reduced) (Fig. 2d). This rapid reduction of Fd is likely due to the electron transport from PSI. After that, the reduction level of Fd was maintained from 2 to 10 ms (Fig. 2d). This means that the retarded electron donation from PSI to Fd by the photo-reduction/oxidation cycle of P700 was almost equal to the electron flow from Fd to FNR, thioredoxin, or  $O_2$ . Afterward, Fd was reduced to 100% in 100 ms, which corresponded to the time scale of the decrease of  $P700^+$  (Fig. 2a). Therefore, electrons produced at PSII flowed into Fd via PSI and accumulated in Fd-pool mainly because of the inactivated FNR under the dark situation. In the third application of SP illumination, the same kinetics as the first SP application was obtained (Fig. 2c, f).

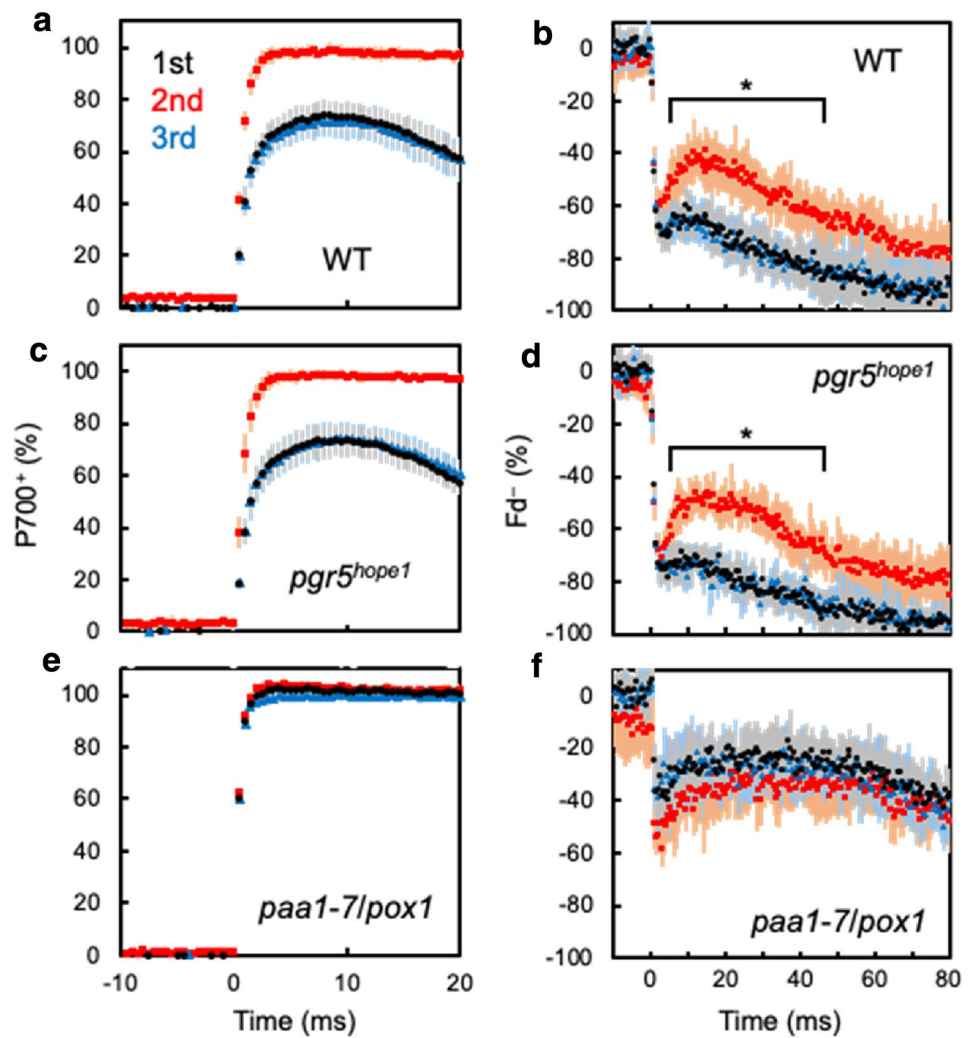
3 s after FR and ST illumination, most of  $P700^+$  returned to the ground state (5% left) while 45–55% of PC was still oxidized (Fig. 2b, e). In this situation, P700 was rapidly oxidized to nearly 100% within the first 2 ms during SP illumination (Fig. 2e). This was due to the lack of electrons in the donor side of PSI (PC and Cyt *f*) by the pre-illumination of FR light. Since P700 was oxidized to 60% in the same time-scale under dark-adapted states, the effects of the electron-donation from PC on the kinetics of  $P700^+$  could not be ignored even within 2 ms from the SP application. Moreover, the sharp decrease of  $P700^+$  after 10 ms was relieved. It took 200 ms for  $P700^+$  to reach nearly 0%,

while it took half the time when PC was fully reduced (first/third SP illumination) (Fig. 2a, b). Following the SP-method,  $Y(I)$  in this situation was 0.9–0.95 which was significantly higher than that in the first SP application (Fig. 3). However, the SP-induced reduction of Fd, especially the initial peak of  $Fd^-$ , showed no difference between the first and second SP applications (Figs. 2e, 4b). Further, the reduction of Fd was suppressed during 5–50 ms of the SP illumination when compared to the reduction kinetics of Fd by the first SP illumination ( $p < 0.05$ ). The oxidation of Fd during 2–10 ms clearly showed that electron donation to Fd from PSI was severely suppressed because of the lack of the electron donor of PSI, reduced PC and reduced Cyt *f*. In other words, the limitation of the electron donation to PSI also contributed to the suppression of the reduction of the Fe-S cluster components located in PSI, as well as the oxidation of P700. These results suggest that  $Y(I)$  value can be easily misestimated depending on the oxidation level of PC.

### The kinetics of oxidized P700 while the saturated pulse illumination in the P700-oxidation mutants

It was previously reported that in the mutants lacking proton gradient regulation 5 (PGR5),  $Y(I)$  showed a closer/lower value when compared to  $Y(II)$  than in WT (Kono et al. 2014; Yamori et al. 2016). Therefore, it has been considered that PGR5 is related to the extra electron flow at PSI observed in WT plants (Kono et al. 2014; Kono and Terashima 2016; Yamori et al. 2016). Previously, another PGR5-deficient

**Fig. 4** The comparison of the kinetics of oxidized P700 (a, c, e) and reduced ferredoxin ( $\text{Fd}^-$ ) (b, d, f) during the saturated pulse (SP) illumination among the first (black symbols), second (red symbols), and third (blue symbols) SP application in wild-type (a, b), *pgr5<sup>hope1</sup>* (c, d), and *paa1-7/pox1* (e, f). Data are shown as average values with SD (thin colored lines of each component). The maximal redox changes of P700, PC, and Fd were determined as shown in Figs. S4 and S5, and each signal was normalized by those values. SP illumination was applied in 0 ms for 300 ms, and the kinetics of P700 in—10 ms to 20 ms and Fd in—10 ms to 80 ms were shown. Asterisks in panel b and d show that in 5–50 ms, the reduction levels of Fd were significantly different between the first and the second SP illumination at over 90% data points ( $p < 0.05$ ). The number of biological replicates is 6 and each signal was obtained by averaging 6 sets of measurements



mutant (*pgr5<sup>hope1</sup>*) was isolated, which showed retarded degradation of chlorophyll fluorescence in photosynthetic induction phases under 2 kPa  $\text{O}_2$ / 40 Pa  $\text{CO}_2$  condition (Wada et al. 2021). In *pgr5<sup>hope1</sup>* mutants, P700 cannot be oxidized under actinic light (especially high-light intensity regions), which is the same phenotype as *pgr5-1* mutants reported in Munekage et al. (2002). It was reported that in the mutants lacking PGR5, there were some malfunctions in “photosynthetic control” system which contributes to the downregulation of the electron flux to PSI resulting in the oxidation of P700 (Fig. S1) (Suorsa et al. 2012, 2013, 2016; Tikkanen et al. 2012, 2015). Moreover, we isolated another P700-oxidation mutant from ethyl methane sulfonate (EMS) treated *A. thaliana*, *paa1-7/pox1*, which showed the slow reduction of P700<sup>+</sup> during SP illumination in the darkness (Fig. S2). In *paa1-7/pox1* mutants, there is a single nucleotide substitution in the DNA sequence coding the Cu-transporting P-type ATPase (PAA1) which is located at the chloroplastic envelope, resulting in the nonsense mutation (Fig. S2). As previously reported in Shikanai et al. (2003), in the mutants

defective in PAA1, the amount of PC, for which Cu is essential to function, was significantly decreased (Figs. S2–S4) and showed high oxidation levels of P700 under actinic light (Fig. S1). Using these two mutants related to the oxidation of P700, we estimated Y(I) by the same method above.

In the *pgr5<sup>hope1</sup>* mutants, there was no significant difference in the kinetics of the three electron carriers during SP illumination when compared to WT (Fig. 4c, d). As observed in WT, the increase of P700<sup>+</sup> by SP illumination was divided into fast (~2 ms) and slow (2 ms~) phases in the first and third Y(I)-estimation while P700<sup>+</sup> reached almost 100% in a few milliseconds at the second estimation of Y(I) when PC was oxidized (Fig. 4c). The Y(I) values were estimated to be 0.7–0.8 for dark-adapted state (first/third SP) and 0.95 for PC-oxidized situation (second SP) (Fig. 3). Moreover, *pgr5<sup>hope1</sup>* also showed similar kinetics of the reduction of Fd during each SP illumination as WT (Fig. 4d, Fig. S6). The transient oxidation of Fd observed in 2–10 ms during SP illumination was also enhanced by PC oxidation (Fig. 4d). These results mean that also in *pgr5<sup>hope1</sup>*, Y(I) value could



be overestimated for the same reasons as WT. However, *pgr5<sup>hope1</sup>* is defective in the limiting system of electron flow at the donor side of PSI under AL, as previously reported in *pgr5-1* mutants (Suorsa et al. 2012). Therefore,  $Y(I)$  values under AL, especially in  $CO_2$  limited or high light intensity conditions, would be less affected by the donor side limitation of the electron flow than in WT.

In *paal-7/pox1*, the amount of photo-oxidizable PC was almost zero (Fig. S4). Therefore, it was estimated that the electron flow from PC to PSI was severely suppressed. In *paal-7/pox1* mutants,  $P700^+$  was rapidly oxidized to nearly 100% at 1–2 ms of SP illumination regardless of the timing of the SP application (Fig. 4e). Concerning the reduction kinetics of Fd, there was no significant difference among the three SP applications (Fig. 4f). Fd was rapidly reduced to 40–60% of the total amount within 2 ms of SP illumination. The transient Fd oxidation was prolonged to 30–40 ms while those of WT and *pgr5<sup>hope1</sup>* in second SP illuminations were observed in 2–10 ms (Fig. 4b, d). This result strongly supported the suggestion that the transient Fd oxidation was caused by the retarded electron supply from PSI. After 20 ms from the SP application, Fd was slowly reduced to 100% in 300 ms, whose kinetics were corresponding to that of the reduction of P700 (Fig. S4). This slow reduction of the two components was due to the lack of PC, resulting in the strong suppression of the electron donation to PSI. This result also suggests that the limitation of electron flow at the donor side of PSI leads to the rapid oxidation of P700 by SP illumination, which would cause the overestimation of  $Y(I)$ .

### Dark-interval relaxation kinetics (DIRK) analysis to estimate the electron flux at PSI

We observed the uncertain  $Y(I)$  values obtained by SP application for quantitative usage (Figs. 2, 3, 4). Next, we verified another method for the estimation of the electron flux at PSI in wheat leaves by evaluating the turnover rate of P700 under steady-state photosynthesis. Sacksteder and Kramer (2000) proposed the less invasive method for the estimation of the electron flux, dark-interval relaxation kinetics (DIRK) analysis. In the DIRK method, a short dark interval (100–400 ms) was applied. Assuming the one-way electron transportation, the initial redox changes of P700 by applying a dark-interval would be determined by the two components; the charge separation of the residue of  $P700^*$  under the AL and the electron flux from PC to  $P700^+$  under the AL. In this research, it was assumed that the existence probability of  $P700^*$  under the actinic light did not influence the initial reduction of  $P700^+$ . The existence possibility of  $P700^*$  has been evaluated as the parameter of  $Y(NA)$ , or the non-photo-oxidizable P700 by SP illumination. Considering that  $Y(I)$  values were easily misestimated,  $Y(NA)$  value would also be an unreliable parameter, because  $Y(NA)$  is

calculated as  $[1 - Y(I) - Y(ND)]$ . Therefore, we cannot evaluate the existence probability of  $P700^*$ . Moreover, the electron donation to the acceptor side of PSI occurs in pico or nano-second order (Vassiliev et al. 2001) while the acquisition point of the equipment was 100  $\mu s$  per 1 plot (Figs. 5, 6). Therefore, it could be considered that the initial reduction rate of  $P700^+$  (vP700) would correspond to the electron transport rate at PSI under the steady-state photosynthesis.

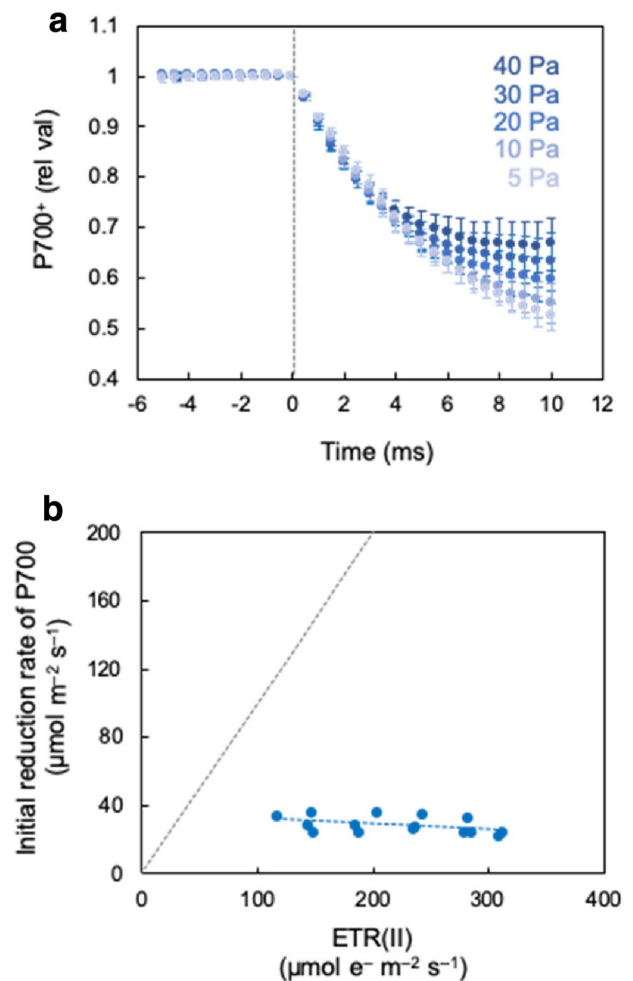


**Fig. 5** **a** The initial reduction kinetics of oxidized P700 during the short dark interval (400 ms of duration) changing the ambient partial pressure of  $CO_2$  (pCO<sub>2</sub>; 40, 30, 20, 10, 5 Pa, approximately) in wheat leaves (*T. aestivum* cv. Norin 61). The intensity of actinic light (AL) was 1,850  $\mu mol$  photons  $m^{-2} s^{-1}$ . The kinetics 5 ms before and 10 ms after the dark application were shown. Data plots and the error bars show the means  $\pm$  SD ( $n=3$ ). **b** The comparison of the turnover rates of P700 in each pCO<sub>2</sub> estimated from the DIRK analysis and the electron transport rate at PSII [(ETR(II)) measured by chlorophyll fluorescence]. The turnover rate of P700 was calculated by multiplying the relative initial reduction rate and the P700 contents in leaves (see “Materials and methods”). The black broken line shows the 1: 1 line of the turnover rate of P700: ETR(II). The blue broken line was arbitrarily drawn to show the trend of the data. The number of biological replicates is 3 and each signal was obtained by averaging 60 sets of dark-interval application

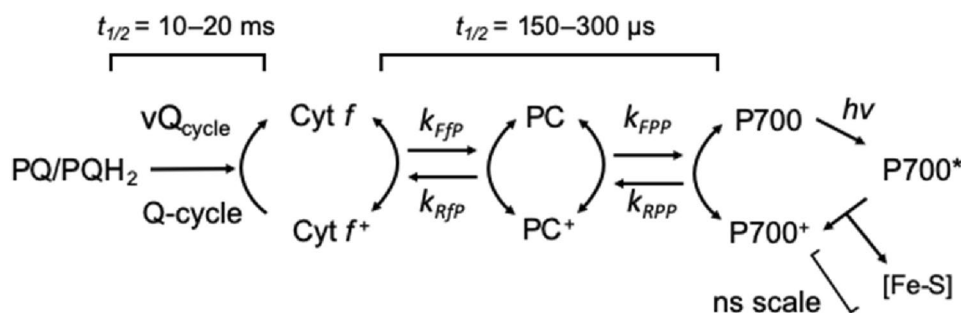


**Fig. 6** The simplified model of photosynthetic electron reaction from plastoquinone-pool to the acceptor side of PSI. The reaction rate of the Q-cycle was defined as  $vQ_{\text{cycle}}$ . The reduction of oxidized PC ( $PC^+$ ) by Cyt  $f$  was determined by the rate constant of  $k_{FFP}$ , and the reverse reaction (oxidation of PC by Cyt  $f^+$ ) was determined by  $k_{RFP}$ . The reduction of  $P700^+$  by PC was defined by  $k_{FPP}$  and the reverse

reaction was by  $k_{RPP}$ . It was reported that the half time of the oxidation of  $PQH_2$  by Cyt  $b_6f$  complex was 10–20 ms, which was the slowest in the photosynthetic reduction/oxidation reactions. The half time of the electron transport reaction from  $P700$  to Fd via  $A_0$ ,  $A_1$ ,  $F_A/F_B$ , and  $F_X$  is fast enough to be ignored

In Fig. 5a, we showed the reduction kinetics of  $P700^+$  under the different ambient partial pressure of  $CO_2$  ( $pCO_2$ ) from 40 to 5 Pa obtained by Dual-KLAS/NIR. We observed few differences in the initial reduction rate of  $P700$  among the different  $pCO_2$  (Fig. 5a), while the oxidation levels of  $P700$  showed a variation from 30 to 60% (Data not shown). We measured the amount of the  $P700$  content in the leaves after the measurements and calculated the turnover rate of  $P700$  ( $vP700$ ). Interestingly,  $vP700$  was significantly lower than electron transport rate at PSII (Fig. 5b). This result indicated that the equilibrium reaction between  $P700$  and PC cannot be ignored. Furthermore, the evaluations of the electron flux in PSI, as  $Y(I)$  and/or the turnover rate of  $P700$ , do not reflect the electron flux at PSI.

## Discussion

In the present research, it turned out that the  $Y(I)$  value was easily misread depending on the oxidation levels at the donor side of PSI (Fig. 3). Even under the dark situation, where it was not necessary to consider any complicated regulations of the photosynthetic electron transport reactions and the capacity of the electron consumption by the CBB cycle,  $Y(I)$  showed different values in the range of 0.1–0.2 depending on the capacities of the electron donation to PSI at the upstream side of PSI. Even in *pgr5<sup>hope1</sup>*, which showed much lower values of  $Y(I)$  than that of  $Y(II)$  (Fig. S1), the kinetics of  $P700^+$  during the SP illumination was significantly different between the dark and PC-oxidized conditions. This result suggested that the lowered  $Y(I)$  value in *pgr5<sup>hope1</sup>* under the steady-state photosynthesis would be caused by the malfunction of the regulation system of the electron flow at the donor side of PSI. Previously,  $Y(I)$  has been treated as the existence probability of the ground state of  $P700$ , or the effective quantum yield of PSI, just as  $Y(II)$ . However,

since the  $Y(I)$  value could be easily misestimated even under dark situations, it is suspicious that  $Y(I)$  can be treated as the quantitative parameter as  $Y(II)$ , although situations are more complicated under AL where the electron consumption by CBB cycle and regulations of electron flow affect the kinetics of the  $P700^+$  during the SP illumination. Importantly, even within a few milliseconds of the SP illumination, the  $P700$  photo-reduction/oxidation cycle is driving to reach another steady-state under the light intensity of SP illumination. Therefore, the kinetics of  $P700^+$  by SP application is always determined by the balance between the influx from the donor side of PSI and the outflux to the acceptor side of PSI. Further,  $Y(NA)$ , calculated as  $1 - Y(I) - Y(ND)$ , also could be said not to be a quantitative parameter. Both  $Y(I)$  and  $Y(NA)$  are obtained by applying the SP illumination. Therefore, these two parameters depend on the balance of the influx and outflux in PSI under the light intensity of SP illumination, and do not reflect the state of the  $P700$  photo-redox cycle under the steady-state photosynthesis. This suggestion was strongly supported by the fact that  $Y(NA)$  showed higher values in low light intensity conditions than in high light intensity (Fig. S1). It can be estimated that the excessive  $Y(I)$  compared to  $Y(II)$  observed in the low  $pCO_2$  and the high light intensity conditions is caused by the enhanced donor side limitation of the electron flow caused by the photosynthetic control, RISE, or other undiscovered mechanisms.

Although it is hard to utilize  $Y(I)$  and  $Y(NA)$  as quantitative parameters, it would be possible to use them as qualitative parameters. For example, oxidation of  $P700$  does not occur in two situations. One is where the regulation of the electron flow does not function because the electron transport reaction is the rate-limiting step such as low light intensity, high  $CO_2$  conditions. The other is where photosynthesis proceeds with a strong limitation at the acceptor side of PSI, such as low  $CO_2$  and  $O_2$ , and some kinds of nutrition

deficient conditions. In the former situations, the  $Y(I)$  values are high while  $Y(NA)$  is low, and vice versa in the latter situations. It is useful to estimate whether the mutants or wild-type plants exposed to treatments would be influenced on the acceptor side or the donor side of PSI. Previously, it was reported that essential nutrient deficiencies influence the photosynthetic parameters including  $Y(I)$  and  $Y(NA)$  in sunflower plants (Ohnishi et al. 2021), which indicated the usage of these parameters as the bio-marker. Even in such cases, it is important to keep in mind that these parameters are determined by the balance of the influx and outflux of the electrons through P700 photo-redox cycle under the SP illumination.

It is hard to estimate the electron flux at PSI by applying SP illumination. We verified another method, DIRK analysis for the evaluation of the electron flux at PSI (Fig. 5). However, the turnover rate of P700 estimated from the combination of the DIRK analysis and quantitative analysis was significantly smaller when compared to the electron flux at PSII estimated from the chlorophyll fluorescence analysis (Fig. 5). This result suggested that the equilibrium reaction among the electron carriers could not be ignored in vivo. In Sacksteder and Kramer (2000), the authors constructed the photosynthetic electron flow model including the equilibrium reaction among Cyt *f*, PC, and P700. They performed the “summation method” for estimating the electron flux, literally summarizing the initial redox change rate of P700 (vP700), PC (vPC), and Cyt *f* (vCyt *f*) by DIRK analysis. Taking the reverse reactions among three carriers into account, the initial redox change rates of each component by dark-interval were determined as follows (Fig. 6);

$$vP700 = k_{FPP}[P700^+][PC] - k_{RPP}[P700][PC^+] \quad (1)$$

$$vPC = k_{FJP}[Cyt\ f][PC^+] - k_{RJP}[Cyt\ f^+][PC] - k_{FPP}[P700^+][PC] + k_{RPP}[P700][PC^+] \quad (2)$$

$$vCyt\ f = vQ_{cycle} - k_{FJP}[Cyt\ f][PC^+] + k_{RJP}[Cyt\ f^+][PC] \quad (3)$$

$k_{Fxx}$  and  $k_{Rxx}$  are the rate constants of the forward and reverse reactions, respectively.  $k_{XPP}$  and  $k_{XJP}$  are the rate constants of the reactions between PC–P700 and Cyt *f*–PC, respectively.  $vQ_{cycle}$  is the reaction rate of Q-cycle at Cyt *b<sub>6</sub>f* complex.

Therefore, the sum of the Eqs. 1, 2 and 3 is below.

$$v(P700 + PC + Cyt\ f) = vQ_{cycle} \quad (4)$$

Considering that the oxidation of PQH<sub>2</sub> by Cyt *b<sub>6</sub>f* (Q-cycle) is the rate-determining step of the electron transport reaction ( $t_{1/2}$  = 10–20 ms), it could be said that the rate of Q-cycle is equal to the whole electron transport rate. It was reported in Sacksteder and Kramer (2000) that the

ratio of the sum of the initial redox change rates of P700, PC, and Cyt *f* to the net CO<sub>2</sub> assimilation rates in the non-photorespiratory condition (2 kPa O<sub>2</sub>) was 4.8 (e<sup>-</sup>/CO<sub>2</sub>) in tobacco leaves.

It is still uncertain whether the reverse reactions occurred in the steady-state of photosynthesis under AL or not. However, it is also hard to evaluate the electron transport rate at PSI under AL from the turnover rate of the P700 by applying the dark interval. From the relatively slow exponential kinetic of P700<sup>+</sup> in the dark interval, it could be estimated that the contribution of charge recombination to electron flux in PSI would be small, considering the rapid half time of the charge recombination in PSI (30 ns for A<sub>0</sub>, 20 μs for A<sub>1</sub>, and 0.5–2 ms for Fx). Therefore, it would be difficult to conclude how electron flows at PSI from the kinetics of P700<sup>+</sup> when an SP illumination or a dark interval is applied.

**Supplementary Information** The online version contains supplementary material available at <https://doi.org/10.1007/s10265-021-01357-6>.

**Author contributions** CM conceived and designed the experiments; RF performed most of the experiments; MO, YM, and SW performed part of the experiments; RF and MO analyzed the data; RF and CM wrote the manuscript.

**Funding** This work was supported by Core Research for Evolutional Science and Technology (CREST) of Japan Science and Technology Agency, Japan (Grant number JPMJCR15O3 to C. M.).

## Declarations

**Ethics approval and consent to participate** Not applicable.

**Consent for publication** Not applicable.

**Conflict of interest** The authors declare no conflict of interest.

## References

- Baker NR (2008) Chlorophyll fluorescence: a probe of photosynthesis in vivo. *Ann Rev Plant Biol* 59:89–113. <https://doi.org/10.1146/annurev.arplant.59.032607.092759>
- Baker NR, Harbinson J, Kramer DM (2007) Determining the limitations and regulation of photosynthetic energy transduction in leaves. *Plant Cell Environ* 30:1107–1125. <https://doi.org/10.1111/j.1365-3040.2007.01680.x>
- Brestic M, Zivcak M, Kunderlikova K, Allakhverdiev SI (2016) High temperature specifically affects the photoprotective responses of chlorophyll b-deficient wheat mutant lines. *Photosynth Res* 130:251–266. <https://doi.org/10.1007/s11120-016-0249-7>
- Chance B (1972) Principles of differential spectrophotometry with special reference to the dual wavelength method. In: Colowick SP, Kaplan NO (eds) *Methods in enzymology*. Elsevier, Amsterdam, pp 322–336. [https://doi.org/10.1016/0076-6879\(72\)24080-0](https://doi.org/10.1016/0076-6879(72)24080-0)

- Driever SM, Baker NR (2011) The water–water cycle in leaves is not a major alternative electron sink for dissipation of excess excitation energy when CO<sub>2</sub> assimilation is restricted. *Plant Cell Environ* 34:837–846. <https://doi.org/10.1111/j.1365-3040.2011.02288.x>
- Furutani R, Ifuku K, Suzuki Y, Noguchi K, Shimakawa G, Wada S, Makino A, Sohtome T, Miyake C (2020a) P700 oxidation suppresses the production of reactive oxygen species in photosystem I. In: Hisabori T (ed) *Advance in botanical research*. Academic Press, Cambridge. <https://doi.org/10.1016/bs.abr.2020.08.001>
- Furutani R, Makino A, Suzuki Y, Wada S, Shimakawa G, Miyake C (2020b) Intrinsic fluctuations in transpiration induce photorespiration to oxidize P700 in photosystem I. *Plants* 9:1761. <https://doi.org/10.3390/plants9121761>
- Genty B, Harbinson J, Briantais JM, Baker NR (1990) The relationship between non-photochemical quenching of chlorophyll fluorescence and the rate of photosystem II photochemistry in leaves. *Photosynth Res* 25:249–257. <https://doi.org/10.1007/bf00033166>
- Ghashghaie J, Cornic G (1994) Effect of temperature on partitioning of photosynthetic electron flow between CO<sub>2</sub> assimilation and O<sub>2</sub> reduction and on the CO<sub>2</sub>/O<sub>2</sub> specificity of RubisCo. *J Plant Physiol* 143:643–650. [https://doi.org/10.1016/S0176-1617\(11\)81152-1](https://doi.org/10.1016/S0176-1617(11)81152-1)
- Hanawa H, Ishizaki K, Nohira K, Takagi D, Shimakawa G, Sejima T, Shaku K, Makino A, Miyake C (2017) Land plants drive photorespiration as higher electron-sink: comparative study of post-illumination transient O<sub>2</sub>-uptake rates from liverworts to angiosperms through ferns and gymnosperms. *Physiol Plant* 161:138–149. <https://doi.org/10.1111/ppl.12580>
- Hope AB (1993) The chloroplast cytochrome bf complex A critical focus on function. *Biochim Biophys Acta Bioenergy* 1143:1–22. [https://doi.org/10.1016/0005-2728\(93\)90210-7](https://doi.org/10.1016/0005-2728(93)90210-7)
- Kadota K, Furutani R, Makino A, Suzuki Y, Wada S, Miyake C (2019) Oxidation of P700 induces alternative electron flow in photosystem I in wheat leaves. *Plants* 8:152. <https://doi.org/10.3390/plant8060152>
- Kanazawa A, Kramer DM (2002) In vivo modulation of nonphotochemical exciton quenching (NPQ) by regulation of the chloroplast ATP synthase. *Proc Natl Acad Sci* 99:12789–12794. <https://doi.org/10.1073/pnas.182427499>
- Kirchhoff H, Schöttler MA, Maurer J, Weis E (2004) Plastocyanin redox kinetics in spinach chloroplasts: evidence for disequilibrium in the high potential chain. *Biochim Biophys Acta Bioenergy* 1659:63–72. <https://doi.org/10.1016/j.bbabi.2004.08.004>
- Klughhammer C, Schreiber U (1991) Analysis of light-induced absorbance changes in the near-infrared spectral region I. Characterization of various components in isolated chloroplasts. *Z Naturforsch C* 46:233–244. <https://doi.org/10.1515/znc-1991-3-413>
- Klughhammer C, Schreiber U (1994) An improved method, using saturating light pulses, for the determination of photosystem I quantum yield via P700<sup>+</sup>-absorbance changes at 830 nm. *Planta* 192:261–268. <https://doi.org/10.1007/bf01089043>
- Klughhammer C, Schreiber U (2016) Deconvolution of ferredoxin, plastocyanin, and P700 transmittance changes in intact leaves with a new type of kinetic LED array spectrophotometer. *Photosynth Res* 128:195–214. <https://doi.org/10.1007/s11120-016-0219-0>
- Klughhammer C, Kolbowski JR, Schreiber U (1990) LED array spectrophotometer for measurement of time resolved difference spectra in the 530–600 nm wavelength region. *Photosynth Res* 25:317–327. <https://doi.org/10.1007/bf00033173>
- Kono M, Terashima I (2016) Elucidation of photoprotective mechanisms of PSI against fluctuating light photoinhibition. *Plant Cell Physiol*. <https://doi.org/10.1093/pcp/pcw103>
- Kono M, Noguchi K, Terashima I (2014) Roles of the cyclic electron flow around PSI (CEF-PSI) and O<sub>2</sub>-dependent alternative pathways in regulation of the photosynthetic electron flow in short-term fluctuating light in *Arabidopsis thaliana*. *Plant Cell Physiol* 55:990–1004. <https://doi.org/10.1093/pcp/pcu033>
- Livingston AK, Cruz JA, Kohzuma K, Dhingra A, Kramer DM (2010) An *Arabidopsis* mutant with high cyclic electron flow around photosystem I (hcef) involving the NADPH dehydrogenase complex. *Plant Cell* 22:221–233. <https://doi.org/10.1105/tpc.109.071084>
- Makino A, Miyake C, Yokota A (2002) Physiological functions of the water–water cycle (Mehler reaction) and the cyclic electron flow around PSI in rice leaves. *Plant Cell Physiol* 43:1017–1026. <https://doi.org/10.1093/pcp/pcf124>
- Malone LA, Proctor MS, Hitchcock A, Hunter CN, Johnson MP (2021) Cytochrome b<sub>6</sub>f—Orchestrator of photosynthetic electron transfer. *Biochim Biophys Acta Bioenergy* 1862:148380. <https://doi.org/10.1016/j.bbabi.2021.148380>
- Miyake C (2020) Molecular mechanism of oxidation of P700 and suppression of ROS production in photosystem I in response to electron-sink limitations in C3 plants. *Antioxidants* 9:230. <https://doi.org/10.3390/antiox9030230>
- Miyake C, Shinzaki Y, Miyata M, Tomizawa K-i (2004) Enhancement of cyclic electron flow around PSI at high light and its contribution to the induction of non-photochemical quenching of chl fluorescence in intact leaves of tobacco plants. *Plant Cell Physiol* 45:1426–1433. <https://doi.org/10.1093/pcp/pch163>
- Miyake C, Miyata M, Shinzaki Y, Tomizawa K-I (2005) CO<sub>2</sub> response of cyclic electron flow around PSI (CEF-PSI) in tobacco leaves—relative electron fluxes through PSI and PSII determine the magnitude of non-photochemical quenching (NPQ) of chl fluorescence. *Plant Cell Physiol* 46:629–637. <https://doi.org/10.1093/pcp/pci067>
- Munekage Y, Hojo M, Meurer J, Endo T, Tasaka M, Shikanai T (2002) PGR5 is involved in cyclic electron flow around photosystem I and is essential for photoprotection in *Arabidopsis*. *Cell* 110:361–371. [https://doi.org/10.1016/s0092-8674\(02\)00867-x](https://doi.org/10.1016/s0092-8674(02)00867-x)
- Munekage Y, Hashimoto M, Miyake C, Tomizawa K-I, Endo T, Tasaka M, Shikanai T (2004) Cyclic electron flow around photosystem I is essential for photosynthesis. *Nature* 429:579–582. <https://doi.org/10.1038/nature02598>
- Nishio JN, Whitmarsh J (1993) Dissipation of the proton electrochemical potential in intact chloroplasts (II. The pH gradient monitored by cytochrome *f* reduction kinetics). *Plant Physiol* 101:89–96. <https://doi.org/10.1104/pp.101.1.89>
- Ohnishi M, Furutani R, Sohtome T, Suzuki T, Wada S, Tanaka S, Ifuku K, Ueno D, Miyake C (2021) Photosynthetic parameters show specific responses to essential mineral deficiencies. *Antioxidants* 10:996. <https://doi.org/10.3390/antiox10070996>
- Oja V, Eichelmann H, Peterson RB, Rasulov B, Laisk A (2003) Deciphering the 820 nm signal: redox state of donor side and quantum yield of photosystem I in leaves. *Photosynth Res* 78:1–15. <https://doi.org/10.1023/a:1026070612022>
- Rantala S, Lempiäinen T, Gerotto C, Tiwari A, Aro EM, Tikkanen M (2020) PGR5 and NDH-1 systems do not function as protective electron acceptors but mitigate the consequences of PSI inhibition. *Biochim Biophys Acta Bioenergy* 1861:148154. <https://doi.org/10.1016/j.bbabi.2020.148154>
- Rott M, Martins NF, Thiele W, Lein W, Bock R, Kramer DM, Schöttler MA (2011) ATP synthase repression in tobacco restricts photosynthetic electron transport, CO<sub>2</sub> assimilation, and plant growth by overacidification of the thylakoid lumen. *Plant Cell* 23:304–321. <https://doi.org/10.1105/tpc.110.079111>
- Ruuska SA, Badger MR, Andrews TJ, Von Caemmerer S (2000) Photosynthetic electron sinks in transgenic tobacco with reduced amounts of Rubisco: little evidence for significant Mehler reaction. *J Exp Bot* 51(suppl\_1):357–368. [https://doi.org/10.1093/jexbot/51.suppl\\_1.357](https://doi.org/10.1093/jexbot/51.suppl_1.357)



- Sacksteder CA, Kramer DM (2000) Dark-interval relaxation kinetics (DIRK) of absorbance changes as a quantitative probe of steady-state electron transfer. *Photosynth Res* 66:145–158. <https://doi.org/10.1023/a:1010785912271>
- Schreiber U, Klughammer C, Neubauer C (1988) Measuring P700 absorbance changes around 830 nm with a new type of pulse modulation system. *Z Naturforsch C* 43:686–698. <https://doi.org/10.1515/znc-1988-9-1010>
- Sejima T, Takagi D, Fukayama H, Makino A, Miyake C (2014) Repetitive short-pulse light mainly inactivates photosystem I in sunflower leaves. *Plant Cell Physiol* 55:1184–1193. <https://doi.org/10.1093/pcp/pcu061>
- Shaku K, Shimakawa G, Hashiguchi M, Miyake C (2015) Reduction-induced suppression of electron flow (RISE) in the photosynthetic electron transport system of *Synechococcus elongatus* PCC 7942. *Plant Cell Physiol*. <https://doi.org/10.1093/pcp/pcv198>
- Shikanai T, Müller-Moulé P, Munekage Y, Niyogi KK, Pilon M (2003) PAA1, a P-type ATPase of Arabidopsis, functions in copper transport in chloroplasts. *Plant Cell* 15:1333–1346. <https://doi.org/10.1105/tpc.011817>
- Shimakawa G, Miyake C (2021) Photosynthetic linear electron flow drives CO<sub>2</sub> assimilation in maize leaves. *Int J Mol Sci* 22:4894. <https://doi.org/10.3390/ijms22094894>
- Shimakawa G, Shaku K, Miyake C (2018) Reduction-induced suppression of electron flow (RISE) is relieved by non-ATP-consuming electron flow in *Synechococcus elongatus* PCC 7942. *Front Microbiol*. <https://doi.org/10.3389/fmicb.2018.00886>
- Suorsa M, Järvi S, Grieco M, Nurmi M, Pietrzykowska M, Rantala M, Kangasjärvi S, Paakkari V, Tikkanen M, Jansson S, Aro E-M (2012) PROTON GRADIENT REGULATION5 is essential for proper acclimation of Arabidopsis photosystem I to naturally and artificially fluctuating light conditions. *Plant Cell* 24:2934–2948. <https://doi.org/10.1105/tpc.112.097162>
- Suorsa M, Grieco M, Järvi S, Gollan PJ, Kangasjärvi S, Tikkanen M, Aro E-M (2013) PGR5 ensures photosynthetic control to safeguard photosystem I under fluctuating light conditions. *Plant Signal Behav* 8:e22741. <https://doi.org/10.4161/psb.22741>
- Suorsa M, Rossi F, Tadini L, Labs M, Colombo M, Jahns P, Kater Martin M, Leister D, Finazzi G, Aro E-M, Barbato R, Pesaresi P (2016) PGR5-PGRL1-dependent cyclic electron transport modulates linear electron transport rate in *Arabidopsis thaliana*. *Mol Plant* 9:271–288. <https://doi.org/10.1016/j.molp.2015.12.001>
- Tikhonov AN (2018) The cytochrome b<sub>6</sub>f complex: biophysical aspects of its functioning in chloroplasts. *Subcell Biochem* 87:287–328. [https://doi.org/10.1007/978-981-10-7757-9\\_10](https://doi.org/10.1007/978-981-10-7757-9_10)
- Tikkanen M, Grieco M, Nurmi M, Rantala M, Suorsa M, Aro E-M (2012) Regulation of the photosynthetic apparatus under fluctuating growth light. *Philos Trans R Soc Lond B Biol Sci* 367:3486–3493. <https://doi.org/10.1098/rstb.2012.0067>
- Tikkanen M, Rantala S, Aro E-M (2015) Electron flow from PSII to PSI under high light is controlled by PGR5 but not by PSBS. *Front Plant Sci*. <https://doi.org/10.3389/fpls.2015.00521>
- Vassiliev IR, Antonkine ML, Golbeck JH (2001) Iron–sulfur clusters in type I reaction centers. *Biochim Biophys Acta Bioenergy* 1507:139–160. [https://doi.org/10.1016/S0005-2728\(01\)00197-9](https://doi.org/10.1016/S0005-2728(01)00197-9)
- Wada S, Suzuki Y, Miyake C (2020) Photorespiration enhances acidification of the thylakoid lumen, reduces the plastoquinone pool, and contributes to the oxidation of P700 at a lower partial pressure of CO<sub>2</sub> in wheat leaves. *Plants* 9:319. <https://doi.org/10.3390/plant9030319>
- Wada S, Amako K, Miyake C (2021) Identification of a novel mutation exacerbated the PSI photoinhibition in pgr5/pgl1 mutants; Caution for overestimation of the phenotypes in Arabidopsis pgr5-1 mutant. *Cells* 10:2884. <https://doi.org/10.3390/cells10112884>
- Yamori W, Makino A, Shikanai T (2016) A physiological role of cyclic electron transport around photosystem I in sustaining photosynthesis under fluctuating light in rice. *Sci Rep* 6:20147. <https://doi.org/10.1038/srep20147>
- Zhang M-M, Fan D-Y, Murakami K, Badger MR, Sun G-Y, Chow WS (2019) Partially dissecting electron fluxes in both photosystems in spinach leaf disks during photosynthetic induction. *Plant Cell Physiol* 60:2206–2219. <https://doi.org/10.1093/pcp/pcz114>
- Zivcak M, Brestic M, Balatova Z, Drevenakova P, Olsovska K, Kalaji HM, Yang X, Allakhverdiev SI (2013) Photosynthetic electron transport and specific photoprotective responses in wheat leaves under drought stress. *Photosynth Res* 117:529–546. <https://doi.org/10.1007/s11120-013-9885-3>
- Zivcak M, Brestic M, Kunderlikova K, Sytar O, Allakhverdiev SI (2015) Repetitive light pulse-induced photoinhibition of photosystem I severely affects CO<sub>2</sub> assimilation and photoprotection in wheat leaves. *Photosynth Res* 126:449–463. <https://doi.org/10.1007/s11120-015-0121-1>

**Publisher's Note** Springer Nature remains neutral with regard to jurisdictional claims in published maps and institutional affiliations.